BOLETÍN DE LA SOCIEDAD ESPAÑOLA DE CERÁMICA Y VIDRIO XXX (2019) XXX–XXX

BOLETIN DE LA SOCIEDAD ESPAÑOLA DE
Cerámica y Vidrio
www.elsevier.es/bsecv

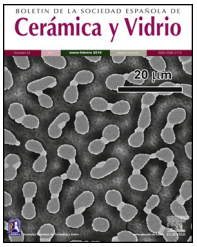

Original

Chitosan and its char as fillers in cement-base composites: A case study

Roberto Nisticò[a,*], *Luca Lavagna*[b], *Daniele Versaci*[b], *Pavlo Ivanchenko*[c,d], *Paola Benzi*[c,e]

[a] *Independent Researcher, Via Borgomasino 39, Torino 10149, Italy*
[b] *Polytechnic of Torino, Department of Applied Science and Technology DISAT, C.so Duca degli Abruzzi 24, Torino 10129, Italy*
[c] *University of Torino, Department of Chemistry, Via P. Giuria 7, Torino 10125, Italy*
[d] *NIS Centre, Via P. Giuria 7, Torino 10125, Italy*
[e] *CrisDi (Interdepartmental Centre for Crystallography), Via P. Giuria 7, Torino 10125, Italy*

ARTICLE INFO

Article history:
Received 6 August 2019
Accepted 30 October 2019
Available online xxx

Keywords:
Chitosan
Composites
Construction materials
Pyrolysis
Toughness

ABSTRACT

The continuous research of new functional materials combining both advanced properties and increased sustainability has dramatically risen up in the last decades. Instead of searching for new solutions, composites (formed by a combination of already present materials) are subject of different studies due to their capability of merging the advantages of components. Hence, chitosan, a biowaste-derived biopolymer, has been thermally-converted into chars by pyrolysis treatment. Subsequently, both chitosan and its char are introduced into cementitious matrix forming cement-based composites. The analysis of the mechanical properties of these materials evidenced that char-containing composites show an incipient fracture toughness capability, very appealing for possible structural applications.

© 2019 SECV. Published by Elsevier España, S.L.U. This is an open access article under the CC BY-NC-ND license (http://creativecommons.org/licenses/by-nc-nd/4.0/).

El quitosano y su carbón como cargas en compuestos a base de cemento: un caso de estudio

Palabras clave:
Quitosano
Compuestos
Materiales de construcción
Pirólisis
Tenacidad

RESUMEN

La investigación continua de nuevos materiales funcionales que combinan propiedades avanzadas y una mayor sostenibilidad ha aumentado dramáticamente en las últimas décadas. En lugar de buscar nuevas soluciones, los compuestos (formados por una combinación de materiales ya presentes) están sujetos a diferentes estudios debido a su capacidad de fusionar las ventajas de los dos componentes. El quitosano, un biopolímero derivado de residuos biológicos, se ha convertido térmicamente en carbón mediante tratamiento de pirólisis. Posteriormente, tanto el quitosano como su carbón se introducen en una matriz cementosa que forma compuestos a base de cemento. El análisis de las propiedades

* *Corresponding author.*
E-mail address: roberto.nistico0404@gmail.com (R. Nisticò).
https://doi.org/10.1016/j.bsecv.2019.10.002
0366-3175/© 2019 SECV. Published by Elsevier España, S.L.U. This is an open access article under the CC BY-NC-ND license (http://creativecommons.org/licenses/by-nc-nd/4.0/).

Please cite this article in press as: R. Nisticò, et al., Chitosan and its char as fillers in cement-base composites: A case study, Bol. Soc. Esp. Cerám. Vidr. (2019), https://doi.org/10.1016/j.bsecv.2019.10.002

mecánicas de estos materiales puso de manifiesto que los compuestos que contienen carbón muestran una incipiente capacidad de resistencia a la fractura, muy atractiva para posibles aplicaciones estructurales.

© 2019 SECV. Publicado por Elsevier España, S.L.U. Este es un artículo Open Access bajo la licencia CC BY-NC-ND (http://creativecommons.org/licenses/by-nc-nd/4.0/).

Introduction

In recent years, several efforts were realized by researchers for finding new materials with advanced peculiar properties and reduced costs [1–5]. In this context, a great attention has been dedicated to the development of composite materials made by combinations of different materials (acting as either matrix or reinforcing agents/fillers) and merging the best technical characteristics of both components [6–10]. In materials science, numerous studies are devoted to the improvement of the intrinsic properties of materials (i.e., mechanical, thermal, electrical, magnetic, optical, properties and so on) or their workability by introducing one (or more) fillers/additives with specific characteristics [11–14].

The possibility of improving the mechanical performance of cement and concrete (in particular the fracture toughness) by means of nanoscopic and/or microscopic fillers is an interesting research field with promising application in the built of earthquake-resistant and monitoring-enabling cementitious materials [15–17]. Among the different types of fillers, carbonaceous ones are widely investigated due to the possibility of introducing novel advanced properties (e.g., the introduction of graphene in cement favored the development of enhanced electrical conductivity) [18]. Moreover, the introduction into cement of bio-based renewable materials and/or natural fibers derived from animal, vegetal and mineral sources attests itself as a real sustainable alternative choice encourage by the building construction industry [19–22].

To date, chitosan (a biopolymer derived from the processing of shellfish biowaste) [23] is a very promising material due to its chemical structure and physicochemical properties [24]. In detail, chitosan is widely exploited in several scientific fields, such as: wastewater treatments [25–28], agriculture and food processing [29,30], cosmetic industry [31], sustainable packaging (e.g., bioplastics) [32–34], and biomedicine (mostly as drug-delivery system since it is bioresorbable) [35–38]. From the chemical viewpoint, chitosan is an amino-polysaccharide and when thermally-treated under inert/reducing atmosphere (i.e., pyrolysis), it can be easily converted into a N-containing carbonaceous materials (i.e., biochar) [39]. According to previous studies [40–42], several natural biopolymers with analogous structure (i.e., polysaccharides) were successfully converted into chars with residual functionalities trough controlled pyrolysis treatments, and exploited mostly for environmental and energetic uses (e.g., adsorbents for the removal of contaminants from wastewater, CO_2 sequestrating agents from gas phase, cathodes in Li-S batteries).

Therefore, in this study chitosan was converted into valuable chars via controlled pyrolysis. Subsequently, both bio-based materials (namely, chitosan and its char) were used for producing reinforced cementitious composites for structural application. Mechanical tests evidenced promising results and an incipient fracture toughness capability, encouraging future studies devoted to the development of such materials, for instance by using a high performance cement as matrix or adding further carbon fibers as reinforcements in order to promote the mechanical response.

Experimental

Pyrolysis treatment

Pyrolysis of chitosan (CAS 9012-76-4, high molecular weight 310–375 kDa, DD = 75–85%, Aldrich) was performed in a quartz tube reactor (Carbolite MTF 12/38/400) under Ar atmosphere with the following thermal program: ramp from room temperature (RT) to target temperature (either 440 °C or 800 °C, rate: 5 °C min^{-1}), isothermal step 1 h. After the pyrolysis treatment, samples were washed twice with deionized water to remove all soluble residues, and dried overnight at 80 °C in an oven. Chars produced were coded as follows: C440 refers to char obtained after heating at 440 °C, whereas C800 refers to the one heated at 800 °C. Samples preparation is reported in Table 1.

Preparation of the cement-base composites

An American Petroleum Institute (API) oil-well cement Class G (Lafarge North America) was used in this work.

Either chitosan or its char (only C800) were dispersed in deionized water (0.1% by weight of cement, or BWOC as in [17]) with an ultrasonic tip (Vibra-cell™) for 15 min at 100 W. The suspensions were mechanical stirred while cement powder was added into the aqueous medium. The water-to-cement (W/C) ratio selected was 0.45. In this work, dispersant or surfactant agents or other additives were not used. The slurry, composed only by cement and chitosan/char, was then poured into molds. The curing for this category of cement is 24 h at 85 °C and at 100% relative humidity. Prismatic molds of size 20 × 20 × 80 mm were used for building the cement-based composites. Composites were coded as follows: CC refers to the cement-chitosan composite, whereas CC800 refers to the

Table 1 – Samples preparation mix design.

Sample name	Cement (g)	Water (g)	Filler (g)
C0	181.11	81.50	–
CC	181.11	81.50	0.18
CC800	181.11	81.50	0.18

Please cite this article in press as: R. Nisticò, et al., Chitosan and its char as fillers in cement-base composites: A case study, Bol. Soc. Esp. Cerám. Vidr. (2019), https://doi.org/10.1016/j.bsecv.2019.10.002

cement composite with char C800. Additionally, for the sake of comparison, also bare cement samples were prepared and identified with the acronym C0.

Characterization

Thermo-gravimetric analysis was conducted in a TGA instrument Mettler Toledo 1600, under Ar atmosphere. The analysis was performed on pristine precursor (chitosan) with the following thermal program: heating ramp from 25 °C to 1000 °C (10 °C min^{-1}). The Ar was supplied with a constant flow rate (50 mL min^{-1}).

Field emission scanning electron microscopy (FESEM) micrographs were collected by means of a FESEM Zeiss Merlin. Various micrographs were taken in different areas of the samples analyzed in order to observe the average morphology.

Elemental analysis of precursor and char was carried out in a Thermo FlashEA 1112 CHNS-O analyzer. Average values of three replicas were provided for each measurement.

FTIR spectra were recorded in attenuated total reflectance mode (ATR, equipped with diamond cell for single reflection) by means of a Vector 22 spectrometer (Bruker) equipped with Globar source, DTGS detector and working with 128 scans at 4 cm^{-1} of resolution in the 4000–400 cm^{-1} range. Spectra were recorded directly on powdery samples.

Mechanical properties were measured with a three-point bending test using the procedure prescribed by JCI-S-001-2003. The specimens were tested with a single-column Zwick-Line z050 flexural testing machine with a load cell having a maximum capacity of 1 kN. As described in the literature [43], the tests were performed on notched specimens (notch width: 2 mm, depth: 5 mm, i.e., equal to one fourth of the width of specimen) by controlling the crack mouth opening displacement (CMOD). CMOD was controlled at a fixed displacement rate of 0.005 mm min^{-1} by placing an extensometer on the two sides of the notch. All tests were performed at least on three specimens, and average values were provided.

The flexural strength was calculated by using the standard formula for un-notched bending tests, using the thickness in the notched area. The toughness was calculated by integrating the load-displacement curve as in [43]. Compressive strength tests were conducted on at least three cubic specimens for each sample (size: 20 × 20 × 20 mm) and controlled at a fixed displacement rate of 0.01 mm min^{-1}.

Results and discussion

Chitosan-to-char conversion: a chemical analysis

To evaluate the pyrolysis induced effect on chitosan structure, TGA analysis was performed on chitosan under inert/reducing atmosphere. Fig. 1 reports the TG profile, which presents two main weight losses: the first one at ca. 100 °C due to the loss of physisorbed water molecules (7 wt.%, i.e., chitosan is a hygroscopic material) and the second one in the 250–400 °C range due to the degradation of the polysaccharidic structure with formation of volatiles products [44]. According to the literature [39], pyrolysis of chitosan leads to the formation of H_2O, CO_2, CO, NH_3, CH_3COOH and N-containing heteroaromatic compounds (mostly pyrazines, pyridines and pyrroles). The curve profile evidences also that at higher temperature (>450 °C) the degradation still continues very slowly, with release of CH_4 and consequent formation of a carbonaceous residue (ca. 27 wt.% at 1000 °C) via dehydrogenation mechanism [39].

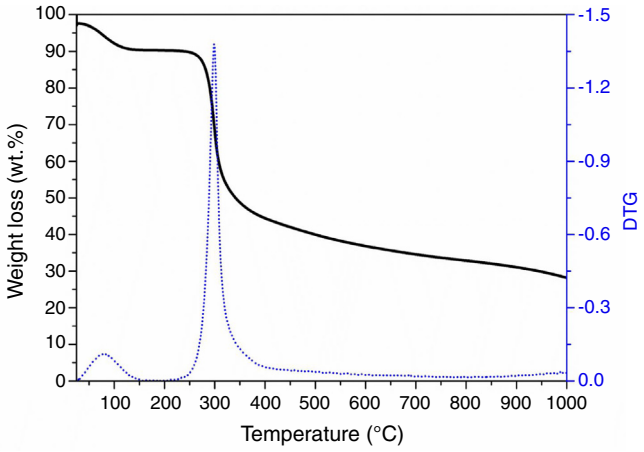

Fig. 1 – TG (black solid) and DTG (blue dotted) analyses of chitosan heated under Ar atmosphere.

For a more detailed comprehension of the chitosan-to-char conversion mechanisms, elemental analysis was performed on either bare chitosan or its chars, sampling at two different target temperatures: namely 440 °C (before) and 800 °C (after the formation of methane documented by the literature for analogous systems) [39]. The analysis revealed a progressive increment of the content of C (from 41.2% to 72.9%) and a reduction of H (from 6.6% to 1.3%). Interestingly, the amount of N increases from pristine chitosan (7.3%) to C440 char (9.8%), while it subsequently decreases to 6.8% for C800. The explanation of this trend is assumable to the fate of N during chitosan pyrolysis. In fact, it has been demonstrated that the amino groups of chitosan can evolve toward either volatile ammonia or being integrated into aromatic structures. Such structures can evolve into a solid N-containing residue (N-doped char) as well as into volatiles N-containing heteroaromatic compounds [39,45]. Therefore, one can easily assume that at high temperatures (800 °C), the loss of residual functionalities is remarkably higher than at low temperature (440 °C). This trend is in agreement with previous study devoted to the pyrolysis of chitin [40] (Table 2).

To deepen the conversion mechanism, ATR–FTIR spectra on chitosan and its chars were collected and results shown in Fig. 2. As evidenced in the figure, the IR spectrum of pristine chitosan revealed the presence of an intense and broad

Table 2 – Elemental analysis for chitosan and its chars (i.e., C440 and C800).

Samples	%C	%H	%N	C/N
Chitosan	41.2	6.6	7.3	5.6
Char (C440)	70.6	3.6	9.8	7.2
Char (C800)	72.9	1.3	6.8	10.8

Please cite this article in press as: R. Nisticò, et al., Chitosan and its char as fillers in cement-base composites: A case study, Bol. Soc. Esp. Cerám. Vidr. (2019), https://doi.org/10.1016/j.bsecv.2019.10.002

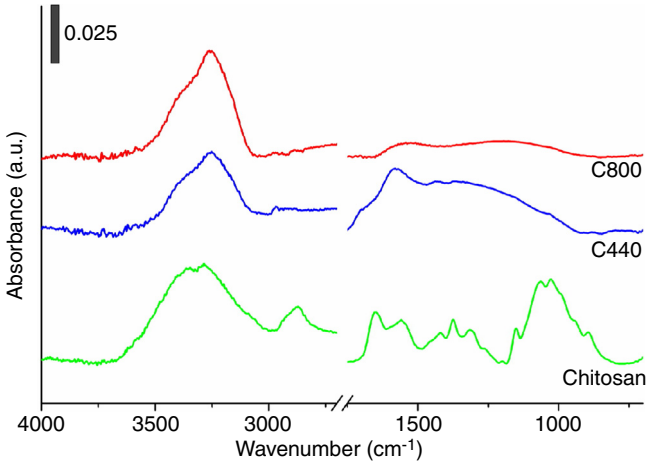

Fig. 2 – ATR–FTIR spectra in the 4000–400 cm^{-1} range of chitosan (green curve), and its chars C440 (blue curve) and C800 (red curve).

band centered at ca. 3440 cm^{-1} attributable to the stretching mode of O–H and N–H functionalities, followed by a small signal in the 2850–2880 cm^{-1} due to stretching mode of aliphatic C-H, the two characteristic signals at ca. 1655 cm^{-1} due to the axial stretching vibration mode of acetamido group (amide I) and the one at ca. 1580 cm^{-1} due to the angular deformation of amino groups, the signals in the 1300–1500 cm^{-1} range commonly assigned to C–N stretching and N–H deformation as well as CH_3 deformation modes, and lastly a broad signal centered at 1000 cm^{-1} due to the skeletal C–O and C–O–C stretching modes. Since chitosan is hydroscopic, the signals at ca. 3440 cm^{-1} and at ca. 1655 cm^{-1} could be associated also to the presence of physisorbed water molecules (O–H stretching and bending modes, respectively). Pyrolysis carried out at high temperatures (both 440 °C and 800 °C) caused the loss of the characteristic glycosidic functional groups with growth of a broad signal in the 1600–1000 cm^{-1} attributable to the formation of carbonaceous C=C and C–C stretching modes, with presence of an IR signal at ca. 3200–3400 cm^{-1} attributable to N–H residual polar functionalities (or still sorbed water molecules) [40]. Additionally, it should be notice that the aliphatic C–H stretching modes at 2850–2880 cm^{-1} are still present in traces in C440, whereas they are absent in the C800 (in agreement with the elemental analysis).

Fig. 3 reports the main morphological differences between precursor prior to perform pyrolysis (Fig. 3A) and at the end of the pyrolysis process (C800, Fig. 3B). Images revealed a rather dense corrugate surface in the case of bare chitosan. On the contrary, pyrolysis treatment favored the formation of surfaces characterized by the presence of debris and defects. The analysis of the cross-section evidenced also the formation of cracks and delamination sites.

Composites production and mechanical tests

Fig. 4 and Table 3 report the results of mechanical tests performed on bare cement (C0) and on composites containing either chitosan (CC) or chitosan-derived char (CC800). Results demonstrate that composites with chitosan possess lower flexural strength compared to reference cement, whereas both toughness and compression strength are not-significantly different between each other. C800-containing materials, instead, show a slight reduction of both flexural strength and compression strength, whereas the relative toughness value is slightly higher than both bare cement and chitosan-containing composites. The loss in terms of flexural strength registered in both cases could be associated to a certain inhomogeneity of samples caused by a difficult interaction between chitosan and its char with the hydrophilic cement paste. On the other hand, the dispersion of the fillers in the cement paste assumes a key role. A bad dispersion of the filler can create defect in the cement matrix composite with a worsening in the mechanical resistance. The presence of functional groups in bare chitosan should favor its integration within the cement matrix, although it must be notice that chitosan is hygroscopic and might compete with the hydration processes involved during the setting step. Moreover, interfacial phenomena are surely the main concern for char-containing composites since char is chemically reduced (and hydrophobic). However, all these issues could be overcome by introducing in the formulation dispersants and compatibilizers (e.g., amphiphilic molecules) or further additives, as well as the chemical functionalization of the char surface.

In general, the analysis of these data (even if not rousing) are still promising since highlights the possibility of successfully introduce chitosan or its char without causing a drastic depletion of the mechanical performances in cement. Furthermore, it must be notice that the experimental value for the toughness in char containing composites is very encouraging. It can be note that the improvement of the toughness response is attributable to the bridging effect of the particles of char dispersed in the cement matrix. In analogy with graphene (see for instance [46,47]), this effect allows a delay

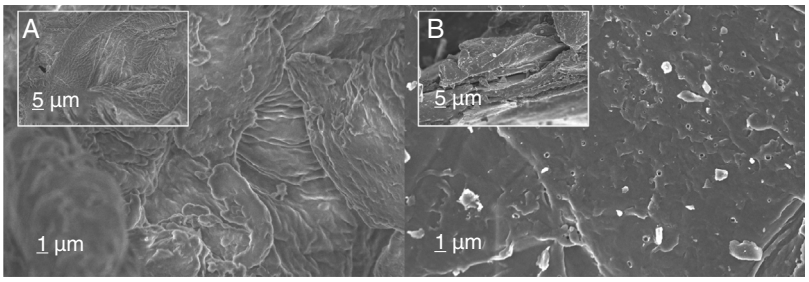

Fig. 3 – FESEM micrographs of bare chitosan (A) and its char C800 (B). Insets refer to the same materials in cross-section at low magnification.

Please cite this article in press as: R. Nisticò, et al., Chitosan and its char as fillers in cement-base composites: A case study, Bol. Soc. Esp. Cerám. Vidr. (2019), https://doi.org/10.1016/j.bsecv.2019.10.002

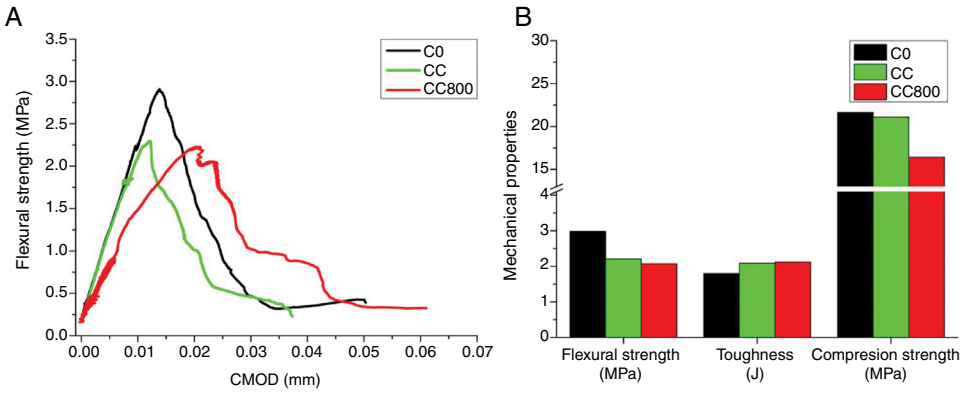

Fig. 4 – Mechanical properties of cementitious composites. Panel A: load–displacement curves for flexural strength. Panel B: mechanical properties (flexural strength, toughness, and compression strength) of C0 (black), CC (green), and CC800 (red).

Table 3 – Mechanical tests behaviors for cementitious composite samples.

Samples	Flexural strength (MPa)[a]	Toughness (J)[a]	Compression strength (MPa)[a]
C0	2.98 ± 0.51	1.80 ± 0.91	21.65 ± 1.13
CC	2.21 ± 0.25	2.09 ± 0.34	21.11 ± 5.22
CC800	2.07 ± 0.13	2.12 ± 0.92	16.43 ± 3.44

[a] Values are means of three measurements ± standard deviation.

in the propagation of micro-cracks if the composite is subjected to an applied stress. The load vs. displacement profile for CC800 confirmed this behavior, demonstrating an incipient fracture toughness capability. Hence, even if these results are only preliminary (and deserve a significant improvement), experiments revealed being an interesting starting point for the development of sustainable toughened cementitious composites.

Conclusions

In this study, chitosan (a biopolymer derived from shellfish industry's biowaste) has been converted into valuable char via pyrolysis. Elemental analysis performed at different pyrolysis conditions revealed a progressive increment of the content of C together with a reduction of H by increasing the process temperature, thus evidencing the progressive chitosan-to-char conversion. The fate of N, instead, results being much more complex, with formation of a N-doping in the residual char, even after pyrolysis at high temperature condition (namely, 800 °C). These results are in agreement with the analysis of the ATR–FTIR spectra of bare chitosan and its chars. Furthermore, from the morphological viewpoint, micrographs revealed the formation of debris and defects at the char's surface, with presence of cracks and delamination sites along the materials' cross-section.

Afterwards, both chitosan and its char (obtained after pyrolysis at 800 °C) were dispersed into a cementious matrix to produce cement-based composites. Mechanical tests revealed that composites enriched with chitosan possess lower flexural strength compared to reference bare cement, whereas the variation of both toughness and compression strength is negligible. Interestingly, by introducing the chitosan-derived char, a slight reduction of both flexural strength and compression strength is registered. However, such side effect is encouragingly balanced by a higher toughness value (even higher than bare cement).

The loss in terms of flexural strength registered in both composites is attributable to a certain inhomogeneity caused by interfacial phenomena occurring between fillers (chitosan/char) and the cement matrix. On the contrary, the improvement of the toughness response is attributable to the bridging effect of the filler's particles dispersed in the cement matrix, which caused a delay in the propagation of micro-cracks when the composite is subjected to an applied stress.

In general, even if the results here discussed are only preliminary, experiments revealed that composite containing the chitosan-derived char evidenced an incipient fracture toughness capability, which is an interesting starting point for further studies on toughness materials.

REFERENCES

[1] N. Nitta, F. Xu, J.T. Lee, G. Yushin, Li-ion battery materials: present and future, Mater. Today 18 (2015) 252–264, http://dx.doi.org/10.1016/j.mattod.2014.10.040.
[2] N. Li, S. Huang, G. Zhang, R. Qin, W. Liu, H. Xiong, G. Shi, J. Blackburn, Progress in additive manufacturing on new materials: a review, J. Mater. Sci. Technol. 35 (2019) 242–269, http://dx.doi.org/10.1016/j.jmst.2018.09.002.
[3] N. Supanchaiyamat, K. Jetsrisuparb, J.T.N. Knijnenburg, D.C.W. Tsang, A.J. Hunt, Lignin materials for adsorption: current trend, perspectives and opportunities, Bioresour. Technol. 272 (2019) 570–581, http://dx.doi.org/10.1016/j.biortech.2018.09.139.
[4] D. Palma, A. Bianco Prevot, L. Celi, M. Martin, D. Fabbri, G. Magnacca, M.R. Chierotti, R. Nisticò, Isolation,

Please cite this article in press as: R. Nisticò, et al., Chitosan and its char as fillers in cement-base composites: A case study, Bol. Soc. Esp. Cerám. Vidr. (2019), https://doi.org/10.1016/j.bsecv.2019.10.002

characterization, and environmental application of bio-based materials as auxiliaries in photocatalytic processes, Catalysts 8 (2018) 197, http://dx.doi.org/10.3390/catal8050197.
[5] P.S. Humbert, J. Castro-Gomes, CO_2 activated steel slag-based materials: a review, J. Clean. Prod. 208 (2019) 448–457, http://dx.doi.org/10.1016/j.jclepro.2018.10.058.
[6] K. Zhang, S. Wang, C. Zhou, L. Cheng, X. Gao, X. Xie, J. Sun, H. Wang, M.D. Weir, M.A. Reynolds, N. Zhang, Y. Bai, H.H.K. Xu, Advanced smart biomaterials and constructs for hard tissue engineering and regeneration, Bone Res. 6 (2018) 31, http://dx.doi.org/10.1038/s41413-018-0032-9.
[7] R. Nisticò, S. Tabasso, G. Magnacca, T. Jordan, M. Shalom, N. Fechler, Reactive hypersaline route: one-pot synthesis of porous photoactive nanocomposites, Langmuir 33 (2017) 5213–5222, http://dx.doi.org/10.1021/acs.langmuir.7b00142.
[8] F. Franzoso, C. Vaca-Garcia, A. Rouilly, P. Evon, E. Montoneri, P. Persico, R. Mendichi, R. Nisticò, M. Francavilla, Extruded versus solvent cast blends of poly(vinyl alcohol-co-ethylene) and biopolymers isolated from municipal biowaste, J. Appl. Polym. Sci. 133 (2016) 43009, http://dx.doi.org/10.1002/app.43009.
[9] X. Yu, J. Zhou, H. Liang, Z. Jiang, L. Wu, Mechanical metamaterials associated with stiffness, rigidity and compressibility: a brief review, Prog. Mater. Sci. 94 (2018) 114–173, http://dx.doi.org/10.1016/j.pmatsci.2017.12.003.
[10] K. Shirvanimoghaddam, S.U. Hamim, M.K. Akbari, S.M. Fakhrhoseini, H. Khayyam, A.H. Pakseresht, E. Ghasali, M. Zabet, K.S. Munir, S. Jia, J.P. Davim, M. Naebe, Carbon fiber reinforced metal matrix composites: fabrication processes and properties, Compos. A: Appl. Sci. Manuf. 92 (2017) 70–96, http://dx.doi.org/10.1016/j.compositesa.2016.10.032.
[11] C. Gonzalez, J.J. Vilatela, J.M. Molina-Aldareguia, C.S. Lopes, J. Llorca, Structural composites for multifunctional applications: current challenges and future trends, Prog. Mater. Sci. 89 (2017) 194–251, http://dx.doi.org/10.1016/j.pmatsci.2017.04.005.
[12] S. Aissou, N. Bouzidi, L. Cormier, E. Bonet-Martines, D. Merabet, Improvement of mechanical and optical properties of Na_2O–CaO–SiO_2 glasses based on dune sand, Bol. Soc. Esp. Cerám. Vidr. 57 (2018) 221–230, http://dx.doi.org/10.1016/j.bsecv.2018.05.002.
[13] Q. Zhang, R. Fang, H. Li, Y. Peng, J. Wang, Tailoring the thermal and mechanical properties of lightweight cement-based composites by macro and micro fillers, Cem. Concr. Comp. 102 (2019) 169–184, http://dx.doi.org/10.1016/j.cemconcomp.2019.04.014.
[14] C. Phrompet, C. Sriwong, C. Ruttanapun, Mechanical, dielectric, thermal and antibacterial properties of reduced graphene oxide (rGO)-nanosized C3AH6 cement nanocomposites for smart cement-based materials, Compos. B: Eng. 175 (2019) 107128, http://dx.doi.org/10.1016/j.compositesb.2019.107128.
[15] S.C. Paul, A.S. van Rooyen, G.P.A.G. van Ziji, L.F. Petrik, Properties of cement-based composites using nanoparticles: a comprehensive review, Constr. Build. Mater. 189 (2018) 1019–1034, http://dx.doi.org/10.1016/j.conbuildmat.2018.09.062.
[16] G. Li, Properties of high-volume fly ash concrete incorporating nano-SiO_2, Cem. Concr. Res. 34 (2004) 1043–1049, http://dx.doi.org/10.1016/j.cemconres.2003.11.013.
[17] L. Lavagna, S. Musso, G. Ferro, M. Pavese, Cement-based composites containing functionalized carbon fibers, Cem. Concr. Comp. 88 (2018) 165–171, http://dx.doi.org/10.1016/j.cemconcomp.2018.02.007.
[18] S. Bai, L. Jiang, N. Xu, M. Jin, S. Jiang, Enhancement of mechanical and electrical properties of graphene/cement composite due to improved dispersion of graphene by addition of silica fume, Constr. Build. Mater. 164 (2018) 433–441, http://dx.doi.org/10.1016/j.conbuildmat.2017.12.176.
[19] C. Martinez-Garcia, B. Gonzalez-Fonteboa, F. Martinez-Abella, D. Carro-Lopez, Performance of mussel shell as aggregate in plain concrete, Constr. Build. Mater. 139 (2017) 570–583, http://dx.doi.org/10.1016/j.conbuildmat.2016.09.091.
[20] O. Onuaguluchi, N. Banthia, Plant-based natural fibre reinforced cement composites: a review, Cem. Concr. Compos. 68 (2016) 96–108, http://dx.doi.org/10.1016/j.cemconcomp.2016.02.014.
[21] H. Du, S.D. Pang, Value-added utilization of marine clay as cement replacement for sustainable concrete production, J. Clean. Prod. 198 (2018) 867–873, http://dx.doi.org/10.1016/j.jclepro.2018.07.068.
[22] M. Frias, H. Savastano, E. Villar, M.I. Sanchez de Rojas, S. Santos, Characterization and properties of blended cement matrices containing activated bamboo leaf wastes, Cem. Concr. Comp. 34 (2012) 1019–1023, http://dx.doi.org/10.1016/j.cemconcomp.2012.05.005.
[23] R. Nisticò, Aquatic-derived biomaterials for a sustainable future: a European opportunity, Resources 6 (2017) 65, http://dx.doi.org/10.3390/resources6040065.
[24] M. Rinaudo, Chitin and chitosan: properties and applications, Prog. Polym. Sci. 31 (2006) 603–632, http://dx.doi.org/10.1016/j.progpolymsci.2006.06.001.
[25] W.S. Wan Ngah, L.C. Teong, M.A.K.M. Hanafiah, Adsorption of dyes and heavy metal ions by chitosan composites: a review, Carbohydr. Polym. 83 (2011) 1446–1456, http://dx.doi.org/10.1016/j.carbpol.2010.11.004.
[26] R. Nisticò, F. Franzoso, F. Cesano, D. Scarano, G. Magnacca, M.E. Parolo, L. Carlos, Chitosan-derived iron oxide systems for magnetically guided and efficient water purification processes from polycyclic aromatic hydrocarbons, ACS Sustain. Chem. Eng. 5 (2017) 793–801, http://dx.doi.org/10.1021/acssuschemeng.6b02126.
[27] S. Sarode, P. Upadhyay, M.A. Khosa, T. Mak, A. Shakir, S. Song, A. Ullah, Overview of wastewater treatment methods with special focus on biopolymer chitin-chitosan, Int. J. Biol. Macromol. 121 (2019) 1086–1100, http://dx.doi.org/10.1016/j.ijbiomac.2018.10.089.
[28] T. Lu, Y. Chen, D. Qi, Z. Cao, D. Zhang, H. Zhao, Treatment of emulsified oil wastewaters by using chitosan grafted magnetic nanoparticles, J. Alloy. Compd. 696 (2017) 1205–1212, http://dx.doi.org/10.1016/j.jallcom.2016.12.118.
[29] P.L. Kashyap, X. Xiang, P. Heiden, Chitosan nanoparticle based delivery systems for sustainable agriculture, Int. J. Biol. Macromol. 77 (2015) 36–51, http://dx.doi.org/10.1016/j.ijbiomac.2015.02.039.
[30] V. Manigandan, R. Karthik, S. Ramachandran, S. Rajagopal, Chitosan applications in food industry, in: A.M. Grumezescu, A.M. Holban (Eds.), Biopolymers for Food Design Handbook of Food Bioengineering, vol. 20, Academic Press, London, UK, 2018, pp. 469–491, http://dx.doi.org/10.1016/B978-0-12-811449-0.00015-3 (Chapter 15).
[31] I.C. Libio, R. Demori, M.F. Ferrao, M.I.Z. Lionzo, N.O. de Silveira, Films based on neutralized chitosan citrate as innovative composition for cosmetic application, Mater. Sci. Eng. C 67 (2016) 115–124, http://dx.doi.org/10.1016/j.msec.2016.05.009.
[32] L.A.M. van der Broek, R.J.I. Knoop, F.H.J. Kappen, C.G. Boeriu, Chitosan films and blends for packaging material, Carbohydr. Polym. 116 (2015) 237–242, http://dx.doi.org/10.1016/j.carbpol.2014.07.039.
[33] M. Mujtaba, R.E. Morsi, G. Kerch, M.Z. Elsabee, M. Kaya, J. Labidi, K.M. Khawar, Current advancements in chitosan-based film production for food technology: a

Please cite this article in press as: R. Nisticò, et al., Chitosan and its char as fillers in cement-base composites: A case study, Bol. Soc. Esp. Cerám. Vidr. (2019), https://doi.org/10.1016/j.bsecv.2019.10.002

review, Int. J. Biol. Macromol. 121 (2019) 889–904, http://dx.doi.org/10.1016/j.ijbiomac.2018.10.109.
[34] J.G. Fernandez, D.E. Ingber, Manufacturing of large-scale functional objects using biodegradable chitosan bioplastic, Macromol. Mater. Eng. 299 (2014) 932–938, http://dx.doi.org/10.1002/mame.201300426.
[35] S.M. Ahsan, M. Thomas, K.K. Reddy, S.G. Sooraparaju, A. Asthana, I. Bhatnagar, Chitosan as biomaterial in drug delivery and tissue engineering, Int. J. Biol. Macromol. 110 (2018) 97–109, http://dx.doi.org/10.1016/j.ijbiomac.2017.08.140.
[36] M.C.G. Pella, M.K. Lima-Tenorio, E.T. Tenorio-Neto, M.R. Guilherme, E.C. Muniz, A.F. Rubira, Chitosan-based hydrogels: from preparation to biomedical applications, Carbohydr. Polym. 196 (2018) 233–245, http://dx.doi.org/10.1016/j.carbpol.2018.05.033.
[37] P. Avetta, R. Nisticò, M.G. Faga, D. D'Angelo, E. Aimo Boot, R. Lamberti, S. Martorana, P. Calza, D. Fabbri, G. Magnacca, Hernia-repair prosthetic devices functionalised with chitosan and ciprofloxacin coating: controlled release and antibacterial activity, J. Mater. Chem. B 2 (2014) 5287–5294, http://dx.doi.org/10.1039/c4tb00236a.
[38] E.I. Rabea, M.E.T. Badawy, C.V. Stevens, G. Smagghe, W. Steurbaut, Chitosan as antimicrobial agent: applications and mode of action, Biomacromolecules 4 (2003) 1457–1465, http://dx.doi.org/10.1021/bm034130m.
[39] I. Corazzari, R. Nisticò, F. Turci, M.G. Faga, F. Franzoso, S. Tabasso, G. Magnacca, Advanced physico-chemical characterization of chitosan by means of TGA coupled on-line with FTIR and GCMS: thermal degradation and water adsorption capacity, Polym. Degrad. Stab. 112 (2015) 1–9, http://dx.doi.org/10.1016/j.polymdegradstab.2014.12.006.
[40] G. Magnacca, F. Guerretta, A. Vizintin, P. Benzi, M.C. Valsania, R. Nisticò, Preparation, characterization and environmental/electrochemical energy storage testing of low-cost biochar from natural chitin obtained via pyrolysis at mild conditions, Appl. Surf. Sci. 427 (2018) 883–893, http://dx.doi.org/10.1016/j.apsusc.2017.07.277.
[41] A. Anceschi, F. Guerretta, G. Magnacca, M. Zanetti, P. Benzi, F. Trotta, F. Caldera, R. Nisticò, Sustainable N-containing biochars obtained at low temperatures as sorbing materials for environmental application: municipal biowaste-derived substances and nanosponges case studies, J. Anal. Appl. Pyroly. 134 (2018) 606–613, http://dx.doi.org/10.1016/j.jaap.2018.08.010.
[42] F. Guerretta, G. Magnacca, F. Franzoso, P. Ivanchenko, R. Nisticò, Sodium alginate conversion into char via pyrolysis at the onset temperature, Mater. Lett. 234 (2019) 339–342, http://dx.doi.org/10.1016/j.matlet.2018.09.127.
[43] S.P. Shah, Determination of fracture parameters (K_{Ic}^{s} and $CTOD_c$) of plain concrete using three-point bend tests, Mater. Struct. 23 (1990) 457–460, http://dx.doi.org/10.1007/BF02472029.
[44] F. Cesano, G. Fenoglio, L. Carlos, R. Nisticò, One-step synthesis of magnetic chitosan polymer composite films, Appl. Surf. Sci. 345 (2015) 175–181, http://dx.doi.org/10.1016/j.apsusc.2015.03.154.
[45] D. de Britto, S.P. Campana-Filho, A kinetic study on the thermal degradation of N,N,N-trimethylchitosan, Polym. Degrad. Stab. 84 (2004) 353–361, http://dx.doi.org/10.1016/j.polymdegradstab.2004.02.005.
[46] K. Gong, Z. Pan, A.H. Korayem, L. Qiu, D. Li, F. Collins, C.M. Wang, W.H. Duan, Reinforcing effects of graphene oxide on Portland cement paste, J. Mater. Civ. Eng. 27 (2015), http://dx.doi.org/10.1061/(ASCE)MT. 1943-5533.0001125, A4014010.
[47] S.V. Bobylev, A.G. Sheinerman, Effect of crack bridging on the toughening of ceramic/graphene composites, Rev. Adv. Mater. Sci. 57 (2018) 54–62, http://dx.doi.org/10.1515/rams-2018-0047.

Please cite this article in press as: R. Nisticò, et al., Chitosan and its char as fillers in cement-base composites: A case study, Bol. Soc. Esp. Cerám. Vidr. (2019), https://doi.org/10.1016/j.bsecv.2019.10.002